Supplement of Hydrol. Earth Syst. Sci., 19, 4081–4098, 2015
http://www.hydrol-earth-syst-sci.net/19/4081/2015/
doi:10.5194/hess-19-4081-2015-supplement

Hydrology and Earth System Sciences
Open Access

Supplement of

Sensitivity of water scarcity events to ENSO-driven climate variability at the global scale

T. I. E. Veldkamp et al.

Correspondence to: T. I. E. Veldkamp (ted.veldkamp@vu.nl)

Supplementary Tables

Table S. 1. Development of (a) the global total population, (b) the global population exposed to water scarcity events (WCI), (c) the global population living in areas sensitive to ENSO driven climate variability, and (d) the global population being exposed to water scarcity events (WCI) & living in areas sensitive to ENSO driven climate variability, between 1961 and 2010 using 5-year averaged values. Numbers between brackets show the values expressed in percentage of the total population. Growth factors represent both the absolute increases as well as the relative increases over time.

	Total Population	Population exposed to water scarcity events(WCI≤1700)	Population sensitive to ENSO driven climate-variability	Population sensitive to ENSO driven climate-variability & exposed towater scarcity events (WCI≤1700)
1961-1965	2.97 billion	0.39 billion (13.2%	1.01 billion (34.1%)	0.14 billion (4.8%)
2006-2010	6.25 billion	2.57 billion (41.1%)	2.41 billion (38.6%)	0.99 billion (15.9%)
Growth factor	2.1	6.6 (3.1)	2.4 (0.4)	6.9 (2.9)

Supplementary Figures

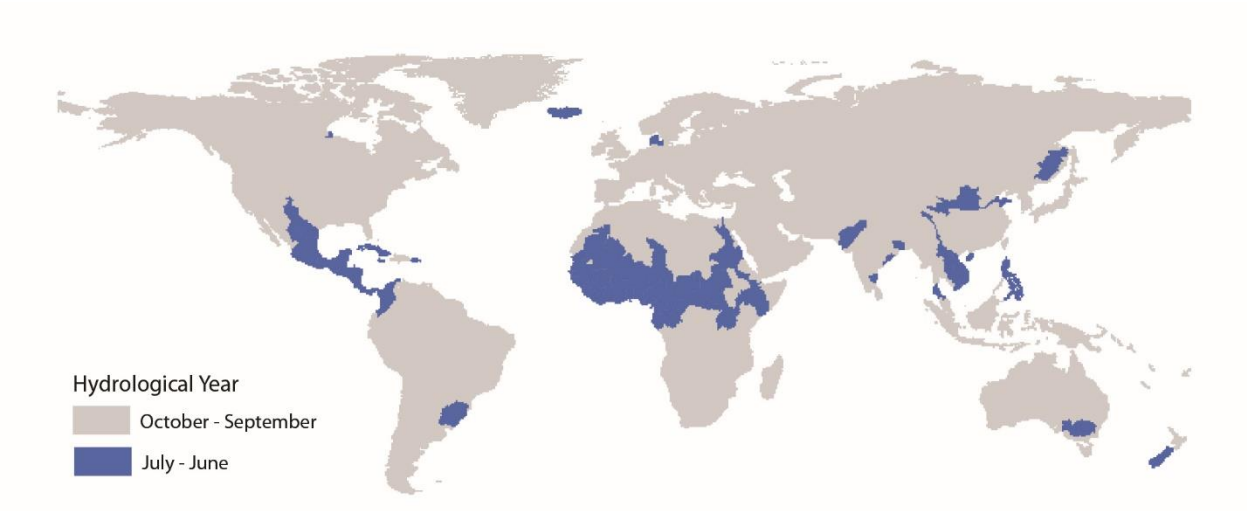

Fig. S 1. Hydrological years used in this study.

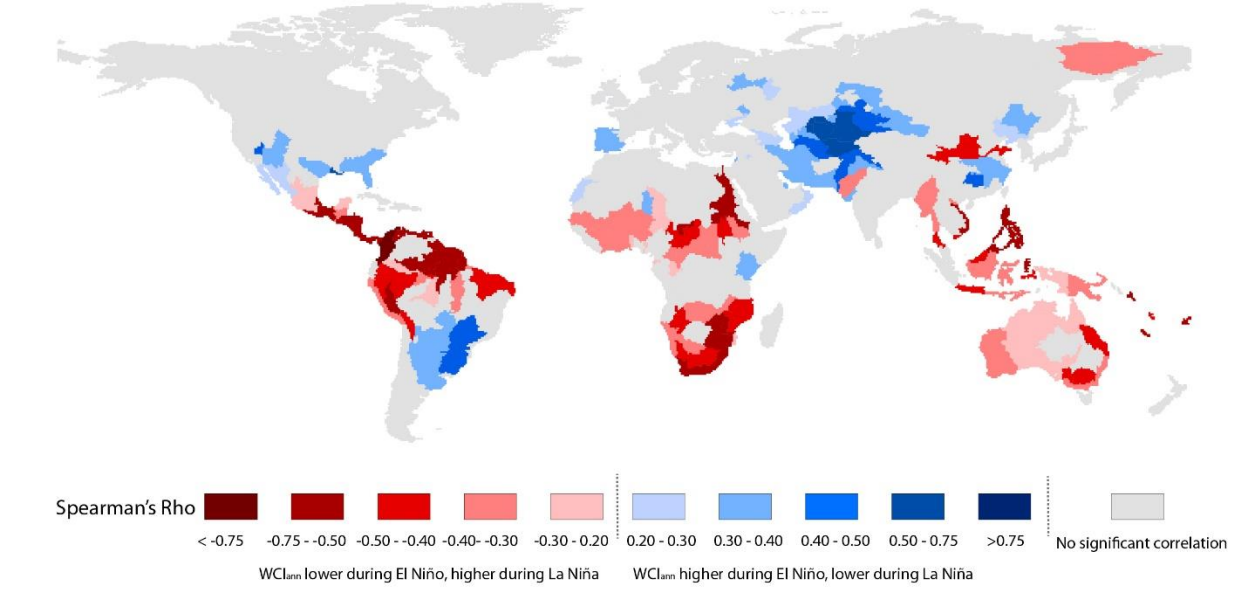

Fig. S 2. Correlation (Spearman's Rho) of yearly water scarcity conditions (WCI), as assessed under fixed socioeconomic conditions, to variations in JMA SST using the 3-monthly period with the highest correlation (JMA $SST_{bestoff}$). Significance was tested by regular bootstrapping (n = 1000, $p \leq 0.05$) and the correlation is only shown for those areas with significant correlations. Positive correlations indicate increases in WCI values (less severe water scarcity conditions) with the JMA $SST_{bestoff}$ index moving towards El Niño values. Negative correlations indicate decreases in WCI values (more severe water scarcity conditions) with the JMA $SST_{bestoff}$ index moving towards El Niño values.

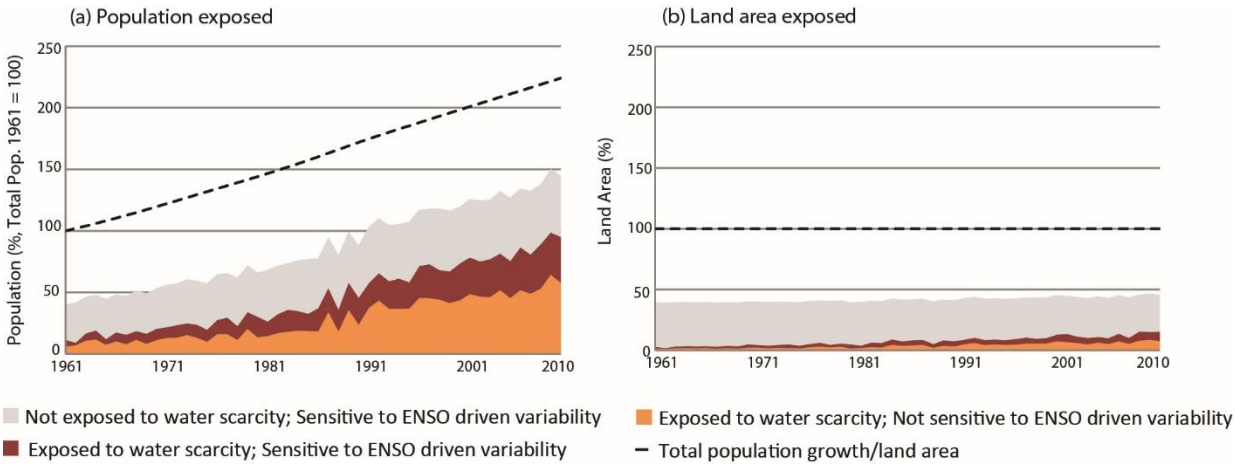

Fig. S 3. Development of population and land-area exposed to water scarcity events and/or being sensitive to ENSO driven climate variability over the period 1961-2010, as estimated with the WCI. Figure S.3.A shows the growth in population living under water scarce conditions and/or living in areas sensitive to ENSO driven climate variability relative to the total growth in global population (set at 100 in 1961). Figure S.3.B shows the increase in land-area exposed to either water scarcity events and/or ENSO driven climate variability relative to the total global land-area (100).

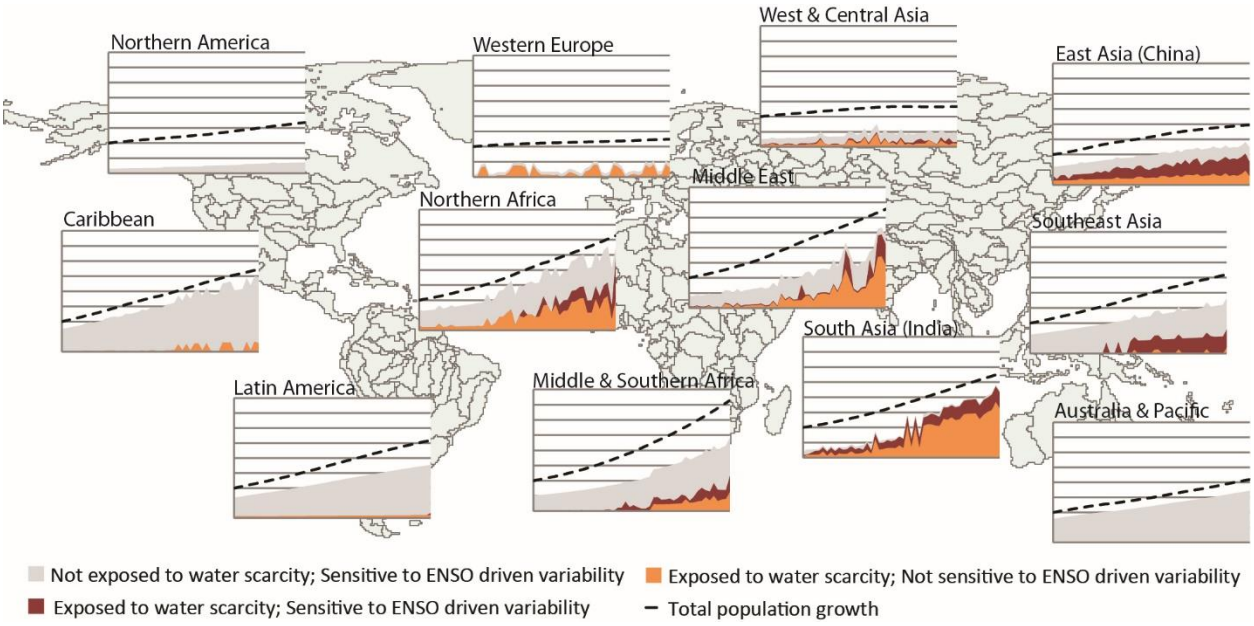

Fig. S 4. Regional variation in developments of population (%) exposed to water scarcity events and/or being sensitive to ENSO driven climate variability over the period 1961-2010, as estimated with the WCI. The figure shows per world region the growth in population living under water scarcity conditions and/or living in areas sensitive to ENSO driven climate variability, relative to the total growth in global population (set at 100 in 1961). Y-axis (% population) ranges from 0 up to 400

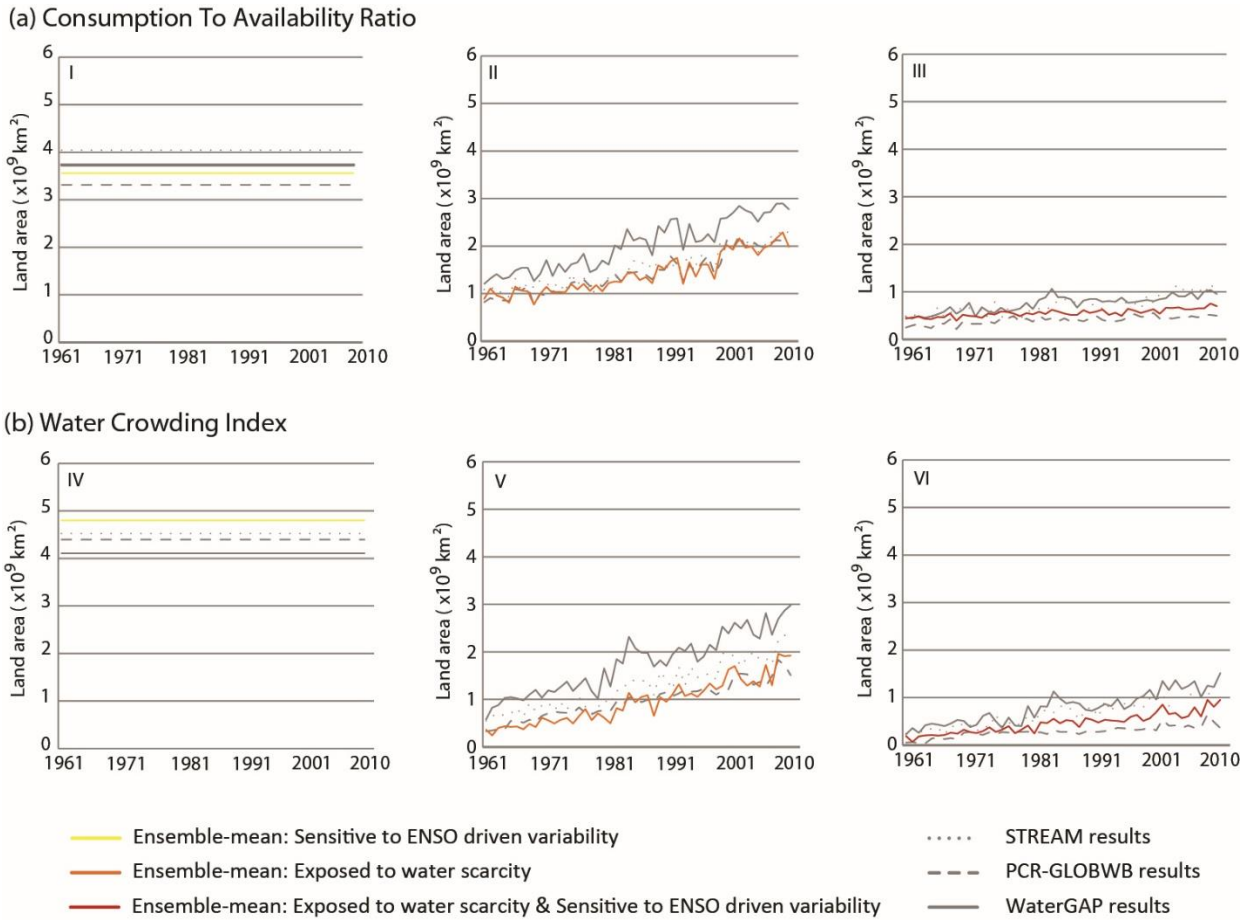

Fig. S 5. Development of the land-area exposed to water scarcity events (WCI) and/or being sensitive to ENSO driven climate variability over the period 1961-2010, as assessed by the individual global hydrological models (STREAM, PCR-GLOBWB, and WaterGAP) and the ensemble-mean. Fig. I and IV show the development in land-area sensitive to ENSO driven climate variability as estimated under the ensemble-mean (yellow) and individual GHMs (grey). Fig. II and V present the increase in land-area exposed to water scarcity events for the ensemble-mean (orange) and individuals GHMs (grey). Fig. III and VI visualize the portion of land-area that is exposed to water scarcity events while it shows at the same time a significant correlation to ENSO driven climate variability for the ensemble-mean (red) and individual GHMs (grey).